

Received March 27, 2019, accepted May 31, 2019, date of publication June 5, 2019, date of current version June 25, 2019.

Digital Object Identifier 10.1109/ACCESS.2019.2920925

Substrate Integrated Plasmonic Waveguide for Microwave Bandpass Filter Applications

LONGFANG YE^{1,2}, YAO CHEN¹, KAI DA XU¹, (Senior Member, IEEE),
WEI WEN LI³, QING HUO LIU⁴, (Fellow, IEEE), AND YONG ZHANG⁵, (Senior Member, IEEE)

¹Institute of Electromagnetics and Acoustics and Department of Electronic Science, Xiamen University, Xiamen 361005, China

²Shenzhen Research Institute, Xiamen University, Shenzhen 518057, China

³Department of Electronic Engineering, Xiamen University, Xiamen 361005, China

⁴Department of Electrical and Computer Engineering, Duke University, Durham, NC 27708, USA

⁵School of Electronic Science and Engineering, University of Electronic Science and Technology of China, Chengdu 611731, China

Corresponding author: Qing Huo Liu (qhliu@duke.edu)

This work was supported in part by the National Natural Science Foundation of China under Grant 61601393, and in part by the Shenzhen Science and Technology Projects under Grant JCYJ20180306172733197.

ABSTRACT In this paper, we numerically and experimentally demonstrate a substrate integrated plasmonic waveguide (SIPW) concept and its application in microwave bandpass filters. This SIPW consists of double arrays of slots etched on the top and bottom metal layers of a substrate integrated waveguide (SIW) to support spoof surface plasmon polariton (SSPP) modes with low and high cutoff frequencies. The simulated results show that by tuning the parameters of the SIPW's unit cell, the dispersion characteristics can be engineered at will. Then, we propose a sharp roll-off microwave bandpass filter based on this SIPW. This filter has a passband from 7.5 to 13.0 GHz with high return loss and low insertion loss. Furthermore, to demonstrate the independent tuning of the passband of the filter, we also design two microwave bandpass filters with passbands of 9.2–13.0 GHz and 7.5–10.5 GHz by decreasing the distance between two rows of via holes and increasing the slot length, respectively. Finally, to experimentally validate the filter designs, we fabricate and measure three prototypes and find that the experimental results are in excellent agreement with the simulations. This SIPW concept may have extensive potential applications in the development of various plasmonic integrated functional devices and circuits.

INDEX TERMS Spoof surface plasmon polaritons, substrate integrated plasmonic waveguide, bandpass filter.

I. INTRODUCTION

Surface plasmon polaritons (SPPs) are a type of electromagnetic (EM) wave mode excited by the interaction between EM field propagating in medium and the free electrons beneath the metal surface [1]. Since its EM fields decay exponentially in the vertical direction to the interface, SPPs are confined around the interface in sub-wavelength scale. Because of the ability to circumvent the diffraction limit, SPPs have been applied in various nano-photonics and optoelectronics [2]–[7]. However, typical frequencies of SPPs correspond to the intrinsic frequencies of metals, which are usually in the visible or ultraviolet region. Owing to the metal intrinsic frequencies cannot be manipulated, the natural SPPs at much

lower frequency regions like microwave or terahertz do not exist.

To realize highly confined EM field at microwave or terahertz bands, Pendry, *et al.* have proposed a concept of spoof surface plasmon polaritons (SSPPs) to mimic the SPPs at optical frequencies [8]. Based on this concept, various microwave and terahertz bulk SSPP waveguides like metal surfaces with textured subwavelength grooves or hole lattices [9]–[13], metal wires with corrugated rings or helical grooves [14]–[17], and domino waveguides [18]–[22] have been theoretically or experimentally investigated. Recently, planar SSPP waveguides have attracted great attention owing to their great potentials in achieving miniaturized and highly-integrated circuits and systems. For example, Cui *et al.* have proposed various planar SSPP waveguides based on rectangular corrugated ultra-thin metal strips for the

The associate editor coordinating the review of this manuscript and approving it for publication was Bora Onat.

compact integrated devices or circuits [23]–[25]. Meanwhile, a lot of planar SSPP waveguides with different unit structures such as single/double side rectangular grooves [26], T-/L-/folded/ spiral stubs [26]–[28], dumbbell units [29] have also been demonstrated to further reduce the sizes of the waveguides. It is found that the asymptotic frequency of the SSPP waveguides can be flexibly controlled by tuning the sizes and shapes of unit structures. Based on these waveguides, various microwave and terahertz devices including antennas [30], [31], power dividers [32], and filters [33] have been developed. Notably, most of the abovementioned SSPP waveguides are made up of modified or complementary structures of planar Goubau lines [25], microstrips [34], slot lines [35], and coplanar waveguides [35], [36].

As we know, substrate integrated waveguide (SIW) is formed in a dielectric substrate by arraying two rows of metallic via holes connecting the upper and lower metal plates to form a dielectrically filled ‘synthesized’ rectangular waveguide [37], [38]. As a class of planar waveguide, SIW possesses many advantages of low insert loss, compact size, easy to be integrated [37]–[40], which has been widely applied to various microwave and millimeter devices and components. Recently, the SSPP concept has been introduced to the SIWs [41]–[47]. For example, Zhang *et al.* designed a passband controllable filter by connecting a traditional SIW and an SSPP waveguide based on anti-symmetrical corrugated metallic strips [41]. Zhu *et al.* proposed a half-space substrate integrated SSPP transmission line using a substrate layer with metalized via holes planted on the ground plane [42]. A slow-wave full-mode SIW and a half-mode SIW are demonstrated in [43], [44]. Moreover, by etching rectangular-/cross-/H-shaped slots on the up-metal layer of SIW [45]–[47], several bandpass filters are also demonstrated. However, these hybrid SSPP-SIW transmission lines and filters are implemented either by using metalized via holes planted on the ground plane or by using etched slots on a single metal layer of SIW, and none of them consider the SSPP unit structures with patterned slots etched simultaneously on double metal layers of SIW.

In this paper, a novel substrate integrated plasmonic waveguide (SIPW) formed by etching double arrays of rectangular slots on both metal layers of SIW is proposed for microwave bandpass filter applications. Firstly, the dispersion characteristics of the SIPW are investigated. It is found that the dispersion relations can be flexibly tuned by manipulating the geometric parameters of the SIPW. The simulated results show that the low and high cutoff (or, asymptotic) frequencies are mainly determined by the distance between two rows of via holes and rectangular slot length, respectively. By utilizing dispersion relations of this SIPW, we design a sharp roll-off bandpass filter based on a microstrip-SIW-SIPW-SIW-microstrip structure with low insertion loss, high return loss in the passband of 7.5–13.0 GHz. The simulated results show that steep rising edge and falling edge of the filter can be controlled independently by tuning the separation between two rows of via holes and the length of the etched

slot in SIPW unit. To demonstrate the filter passband tuning property, we then design two bandpass filters with passbands of 9.2–13.0 GHz and 7.5–10.5 GHz by decreasing distance between two rows of via holes and increasing the slot length, respectively. The measured results are in good agreement with the simulated ones. The proposed SIPW may play an important role in microwave integrated plasmonic systems and circuits.

II. DISPERSION CHARACTERISTICS OF SIPW

The proposed SIPW is composed of an SIW by etching double arrays of patterned slots on both metal layers. Here, we take the rectangular slots as an example to demonstrate the properties of SIPW. The schematic configurations of the top-view of SIPW and its unit cell are depicted in Figs. 1(a) and 1(b), respectively. We choose copper as metal layers with the conductivity (σ) of 5.8×10^7 S/m and the thickness (t_1) of 0.018 mm, and Rogers 5880 as the dielectric substrate with the relative permittivity (ϵ_r) of 2.2, the loss tangent of 0.0009, and the thickness (t_2) of 0.508 mm. The height (h) and width (g) of the rectangular slot are initially set as 8 and 0.2 mm, respectively. Other parameters are set as follows: the width of SIPW $W = 18$ mm, the diameter of metallic via holes $d = 0.6$ mm, the distance between two rows of via holes $a = 14.55$ mm, the spacing of adjacent via holes $s = 1$ mm, the period of SIPW unit cell $p = 2$ mm.

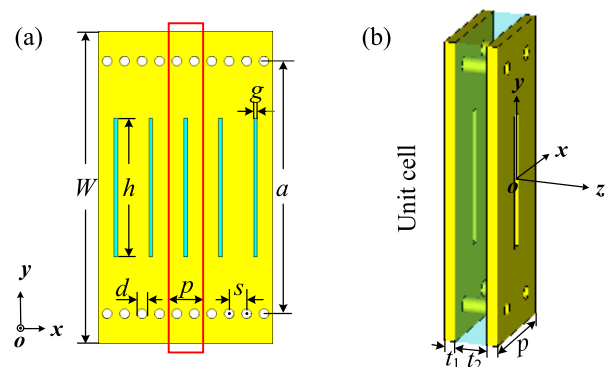


FIGURE 1. Schematic configuration of the SIPW. (a) The top view of the SIPW ($W = 18$ mm, $d = 0.6$ mm, $a = 14.55$ mm, $s = 1$ mm, $p = 2$ mm, $g = 0.2$ mm, $h = 8$ mm, $b = 0.2$ mm). (b) Three-dimensional structure of the unit cell ($t_1 = 0.018$ mm, $t_2 = 0.508$ mm).

To study the properties of the SIPW, we first analyze the dispersion characteristics of the SIPW unit cell. In the numerical simulations, we use the eigenmode solver of CST microwave studio to calculate the dispersion curves. Figure 2(a) shows the comparison of the dispersion curves of the light line, single slotted SIW, and the double-slotted SIW (SIPW). It is found that the dispersion curves of both the single and double slotted SIW deviate far away from the light line, which is as expected from the supported SSPP modes. Meanwhile, SIPW with double slots demonstrates even lower asymptotic frequency compared to the single slotted case, implying higher potential in the development of minimized

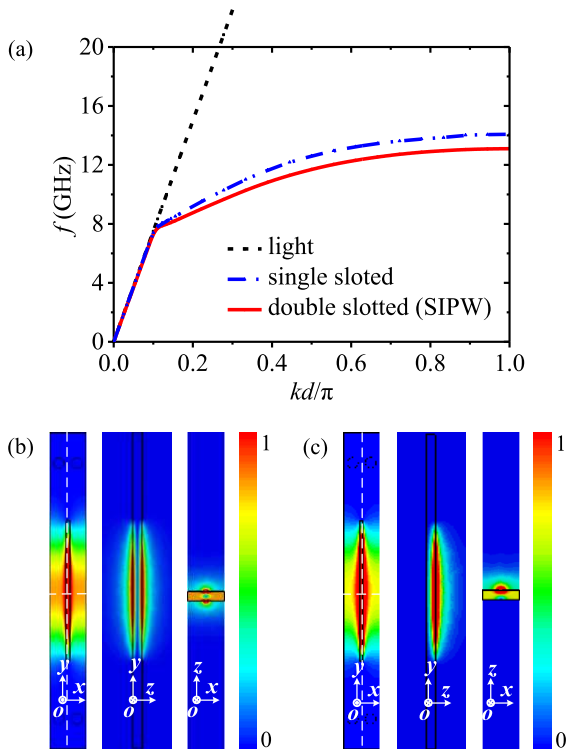


FIGURE 2. Dispersion characteristics and electric field distributions of the SIPW unit cells. (a) Comparison of the dispersion curves of the light line, single slotted SIW, and the double-slotted SIW (SIPW). Normalized electric field distributions for (b) double- and (c) single-slotted unit cells.

microwave devices and circuits. Figures 2(b) and 2(c) depict the normalized electric field distributions for the single and double slotted unit cells. The electric fields of the SIPW strongly concentrate around both slot areas of the structure, which is obviously different from that of single slotted SIW.

The dispersion characteristics of SIPWs can be flexibly tuned by manipulating the waveguide geometric parameters. Figure 3(a) shows the dependence of dispersion relations for the fundamental SPP mode on a ranging from 9 to 14.55 mm while keeping $h = 8$ mm and the rest other parameters fixed as the initial values. It is clear that the low cutoff frequency of SPP mode of the SIPW decreases from 11.7 to 7.5 GHz while keeping the high cutoff (or, asymptotic) frequency almost unchanged as a increases from 9 to 14.55 mm. We find the low cutoff frequency is also approximately equal to the cutoff frequency of conventional SIW, which is determined by

$$f_c = \frac{c}{2\sqrt{\epsilon_r}} \left(a - \frac{d^2}{0.95s} \right)^{-1},$$

where c is the speed of light in free space. Figure 3(b) displays the dispersion relations for different h ranging from 2 to 10 mm with a set as 14.55 mm and other parameters fixed as the initial values. We find that, as h increases from 2 to 8 (10) mm, the asymptotic frequency decreases drastically from 40.4 to 13.1 (10.8) GHz while keeping the low cutoff frequency almost the same. Therefore, the low

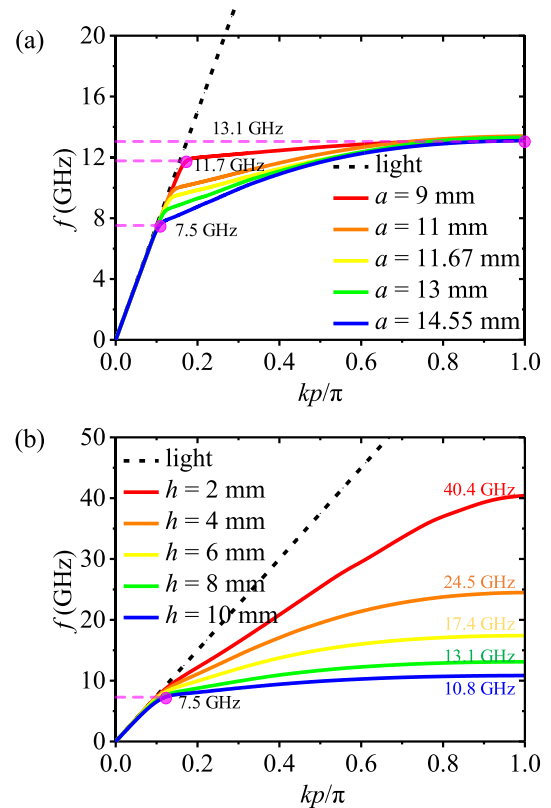


FIGURE 3. Dispersion relations for the fundamental SSPP mode of the SIPW. (a) Dispersion relations for different a ranging from 9 to 14.55 mm while keeping $h = 8$ mm and other parameters fixed as the initial values. (b) Dispersion relations for different h ranging from 2 to 10 mm with the a set as 14.55 mm and other parameters fixed as the initial values.

cutoff frequency and asymptotic frequency of the SIPW are independently determined by a and h , respectively, leading to more design flexibility compared to the conventional SSPP waveguides, which is mainly determined by the effective depth of the corrugation. Obviously, SIPW can be applied in the microwave bandpass SSPP filters by taking the advantages of its dual-cutoff dispersion characteristics of the SSPP mode.

III. DEMONSTRATION OF MICROWAVE BANDPASS SIPW FILTERS

To demonstrate the application of SIPW, we design a sharp roll-off bandpass SIPW filter (model I) at microwave frequencies using a microstrip-SIW-SIPW-SIW-microstrip structure. The top and bottom views of the filter schematics are illustrated in Figs. 4(a) and 4(b), where region I is a broadband microstrip-SIW transition using a connected 50 Ω microstrip-tapered microstrip-SIW structure, and region II is a broadband SIW-SIPW transition made up of an SIW-graded SIPW-SIPW structure. In this SIPW filter, the low and high cutoff (or asymptotic) frequencies are independently determined by the distance between two rows of via holes and rectangular slot length, respectively, as shown in Fig. 3. The microstrip-SIW transition enables the transmitting quasi-TEM mode of microstrip to be smoothly converted

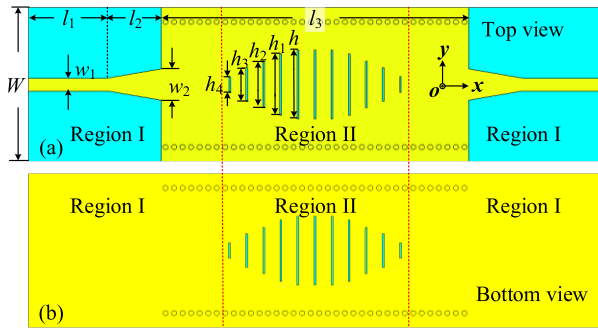


FIGURE 4. Schematic configuration of the proposed SIPW filter (model I). (a) Top view, (b) bottom view. The geometric parameters are set as $l_1 = 9.3$ mm, $w_1 = 1.5$ mm, $l_2 = 6.28$ mm, $w_2 = 3.63$ mm, $l_3 = 36$ mm, $W = 18$ mm, $h_4 = 1.8$ mm, $h_3 = 3.93$ mm, $h_2 = 5.37$ mm, $h_1 = 7.16$ mm, $h = 8$ mm, and $a = 14.55$ mm.

to quasi-TE mode of SIW, and then the graded length of the rectangular slot in the SIW-SIPW transition produces smooth momentum ($p = \hbar k$, where \hbar denotes the reduced Planck constant) and impedance matching to efficiently convert quasi-TE mode of SIW to SSPP mode of SIPW.

In the SIW-SIPW transition design, owing to the wave vector k of the SSPPs in SIPW is far greater than that of quasi-TE mode in SIW, we first set the initial values of graded rectangular slot lengths as $h_i = h - 1.6 i = 8 - 1.6 i$ ($i = 1, 2, 3, 4$). For example, as shown in Fig. 5(a), k increases gradually as the slot length increases under the given frequency of 12 GHz, therefore, allowing smooth momentum matching and mode conversion between SIW and SIPW by using this transition structure. However, with the initial slot lengths, the reflection coefficient S11 of the filter is larger than -10 dB between 11.2 and 12.1 GHz in the passband, as shown in Fig. 5(b), implying certain impedance mismatching of the transition in that frequency range. In order to improve impedance matching and SIPW filter performance, we carry out the parameter optimization and set the optimized geometric parameters as, $l_1 = 9.3$ mm, $w_1 = 1.5$ mm, $l_2 = 6.28$ mm, $w_2 = 3.63$ mm, $l_3 = 36$ mm, $W = 18$ mm, $h_4 = 1.8$ mm, $h_3 = 3.93$ mm, $h_2 = 5.37$ mm, $h_1 = 7.16$ mm, $h = 8$ mm, $a = 14.55$ mm, $d = 0.6$ mm, $s = 1$ mm, $p = 2$ mm, and $g = 0.2$ mm, also shown in the caption of Fig. 4. The material parameters of this filter are the same as those presented above. Figure 5(b) also shows that the frequency responses of the SIPW filter with optimized geometric parameters are improved with $S_{11} < -15$ dB in the whole passband. Furthermore, the comparison of simulated S-parameters of double slotted SIPW filter and the single slotted SIW filter under the same geometric parameters is shown in Fig. 5(c). It is found that the high cutoff frequency of the proposed SIPW filter is about 13 GHz, which is smaller than that about 13.9 GHz of the single slotted SIW filter. In other words, the proposed double slotted structure will require a smaller slot length to achieve the same passband compared to the single slotted structure. These results are in good agreement with the dispersion relations shown in Fig. 2(a).

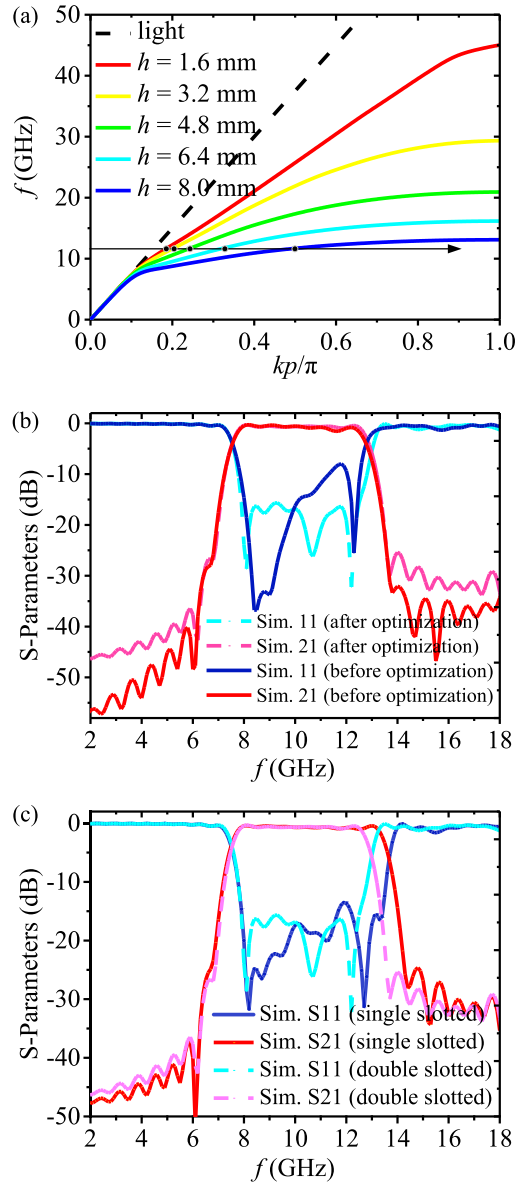


FIGURE 5. (a) Dispersion relations of the proposed SIPW unit cell with different h ranging from 1.6 mm to 8 mm. (b) Comparison of simulated (Sim.) S-parameters between the proposed SIPW filter (model I) with initial graded slot lengths (equal step of 1.6 mm) and the optimized geometric parameters. (c) Comparison of simulated S-parameters of double slotted SIPW filter and the single slotted SIW filter under the same geometric parameters.

The properties of the proposed filter are verified by experimental measurement using a vector network analyzer (Agilent N5230C). A fabricated prototype with two SMA connectors is displayed in Figs. 6(a) and 6(b). The simulated and measured scattering parameters (S-parameters) results are compared in Fig. 6(c). It is found that the simulated transmission coefficient S21 is higher than -1 dB and reflection coefficient S11 is lower than -15 dB in the passband with two sharp roll-offs at 7.5 and 13.0 GHz, which are consistent with the lower cutoff frequency and asymptotic frequency of the SIPW unit cell in Fig. 3. The measured results also show good filtering performance with the same passband and roll-off

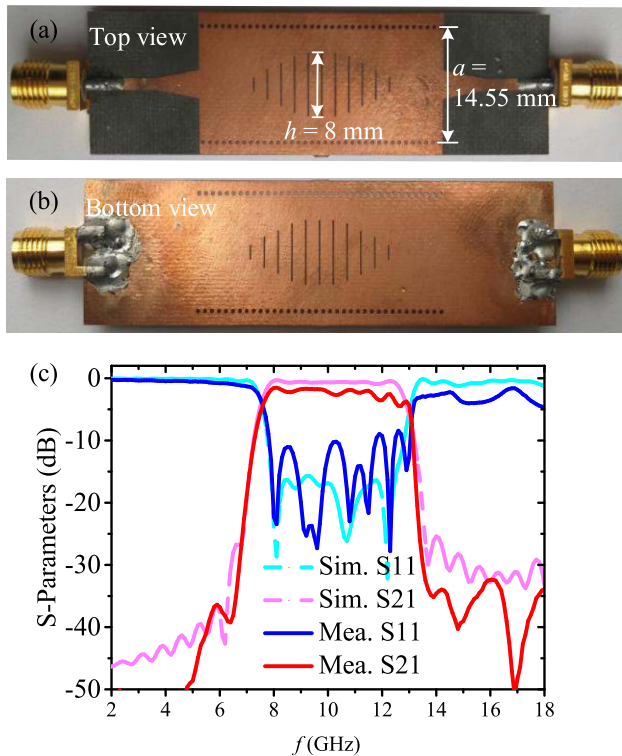


FIGURE 6. Fabricated microwave SIPW filter (model I). (a) Top view and (b) bottom view photographs of the fabricated SIPW filter. (c) Simulated (Sim.) and measured (Mea.) S-parameters of the fabricated SIPW filter.

properties, which verify the effectiveness of the proposed filter design. Moreover, the relative larger insertion loss and higher reflection within the passband of the measured results are mainly caused by the impedance mismatching in the soldering of SMA and fabrication tolerance.

To get more insight into the SIPW filter, we investigate the electric field distributions cut on the xoy plane at 0.1 mm above the top metallic layer. Figure 7(a) shows the normalized field distributions at 4 GHz in the lower stopband. It is clear that the 4 GHz microwaves propagate and reflect back in the microstrip part without transmitting into the SIW region because of the frequency smaller than the lower cutoff frequency of SIW. While, the microwave at 10 GHz within the passband can propagate efficiently through the whole SIPW filter with smooth mode conversion and small loss, as shown in Fig. 7(b). Furthermore, Fig. 7(c) shows the microwave at 16 GHz within the upper stopband is terminated in the graded SIPW part, which can also be predicted from the dispersion relations shown in Fig. 3. These field distributions show a good agreement with the S-parameter results in Fig. 6(c) and provide an intuitionistic verification to SIPW filtering performance.

To study the independent manipulation characteristics of the SIPW passband, we investigate the influence of distance between two rows of via holes (a) and slot length (h) on the frequency responses of SIPW filter. Firstly, we design another two SIPW filters modified from the original filter design (model I) presented above by reducing a

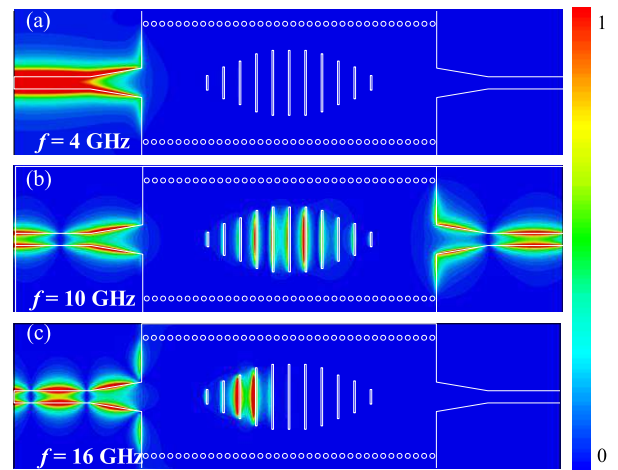


FIGURE 7. The simulated normalized electric field distributions at 0.1 mm above the top metallic layer of SIPW at (a) 4 GHz, (b) 10 GHz, and (c) 16 GHz, respectively.

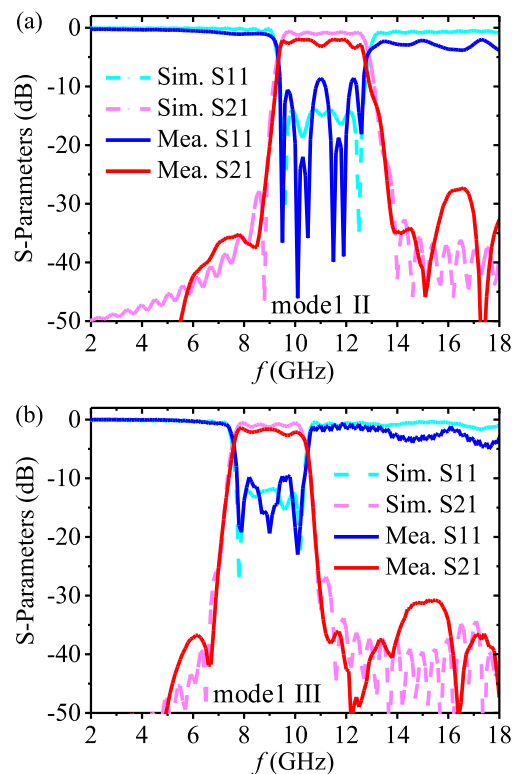


FIGURE 8. The simulated (Sim.) and measured (Mea.) S-parameters of the fabricated SIPW filters (a) model II and (b) model III.

from 14.55 to 11.67 mm while remaining h fixed as 8 mm (model II) and by increasing h from 8 to 10 mm with a fixed as 14.55 mm (model III). The simulated and measured S-parameters of the filter model II and model III, with a good agreement, are presented in Figs. 8(a) and 8(b), respectively. We can observe that as the distance a decreases to 11.67 mm in SIPW filter model II, the lower cutoff frequency increases to 9.2 GHz, leading to a passband of 9.2-13.0 GHz without affecting the higher cutoff frequency. Similarly, in SIPW filter model III, the passband turns to 7.5-10.5 GHz as the upper

cutoff frequency decreases owing to the increasing h . The numerical and experimental results verify that the passband properties can be flexibly tuned independently by adjusting a and h , which are consistent with the dispersion relations shown in Figs. 3(a) and 3(b).

IV. CONCLUSION

We have demonstrated a new SIPW and its application in microwave bandpass filters. The dispersion characteristics of the proposed SIPW unit cell are simulated and analyzed. It is found that the SIPW supports SSPs in the passband between its low cutoff and high cutoff (asymptotic) frequencies. The low cutoff and asymptotic frequencies are mainly determined by the distance a between two rows of via holes and rectangular slot length h , respectively. By using microstrip-SIW-SIPW-SIW-microstrip structure to achieve smooth mode conversion and impedance matching, an original microwave bandpass filter with the passband of 7.5 to 13.0 GHz is designed and tested with good filtering responses. To demonstrate the independent passband tuning properties, another two SIPW filters modified from the original filter are also designed with a passband of 9.2 to 13.0 GHz by reducing a and a passband of 7.5 to 10.5 GHz by increasing h , which are well consistent with the dispersion characteristics for the SIPW. The numerical and experimental results show all the filters possess promising performance with a simple structure, low insertion loss, high return loss, and sharp roll-offs. This SIPW concept not only can be applied in microwave filters but also may have extensive potential applications in the development of various plasmonic integrated functional devices and circuits.

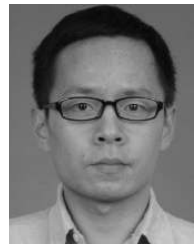
REFERENCES

- [1] W. L. Barnes, A. Dereux, and T. W. Ebbesen, "Surface plasmon subwavelength optics," *Nature*, vol. 424, no. 6950, pp. 824–830, 2003.
- [2] D. K. Gramotnev and S. I. Bozhevolnyi, "Plasmonics beyond the diffraction limit," *Nature Photon.*, vol. 4, no. 2, pp. 83–91, 2010.
- [3] R. Zia, J. A. Schuller, A. Chandran, and M. L. Brongersma, "Plasmonics: The next chip-scale technology," *Mater. Today*, vol. 9, nos. 7–8, pp. 20–27, Jul./Aug. 2006.
- [4] T. W. Ebbesen, C. Genet, and S. I. Bozhevolnyi, "Surface-plasmon circuitry," *Phys. Today*, vol. 61, no. 5, pp. 44–50, May 2008.
- [5] S. Kawata, Y. Inouye, and P. Verma, "Plasmonics for near-field nanoimaging and superlensing," *Nature Photon.*, vol. 3, no. 1, pp. 388–394, 2009.
- [6] E. Ozbay, "Plasmonics: Merging photonics and electronics at nanoscale dimensions," *Science*, vol. 311, no. 5758, pp. 189–193, Jan. 2006.
- [7] A. L. Falk, F. H. L. Koppens, C. L. Yu, K. Kang, N. de L. Snapp, A. V. Akimov, M.-H. Jo, M. D. Lukin, and H. Park, "Near-field electrical detection of optical plasmons and single-plasmon sources," *Nature Phys.*, vol. 5, pp. 475–479, May 2009.
- [8] J. B. Pendry, L. Martín-Moreno, and F. J. García-Vidal, "Mimicking surface plasmons with structured surfaces," *Science*, vol. 305, pp. 847–848, Aug. 2004.
- [9] Z. Ruan and M. Qiu, "Slow electromagnetic wave guided in subwavelength region along one-dimensional periodically structured metal surface," *Appl. Phys. Lett.*, vol. 90, no. 20, May 2007, Art. no. 201906.
- [10] J. J. Wood, L. A. Tomlinson, O. Hess, S. A. Maier, and A. I. Fernández-Domínguez, "Spoof plasmon polaritons in slanted geometries," *Phys. Rev. B, Condens. Matter*, vol. 85, no. 7, Feb. 2012, Art. no. 075441.
- [11] C. L. C. Smith, N. Stenger, A. Kristensen, N. A. Mortensen, and S. I. Bozhevolnyi, "Gap and channeled plasmons in tapered grooves: A review," *Nanoscale*, vol. 7, no. 21, pp. 9355–9386, May 2015.
- [12] F. J. García-Vidal, L. Martín-Moreno, and J. B. Pendry, "Surfaces with holes in them: New plasmonic metamaterials," *J. Opt. A, Pure Appl. Opt.*, vol. 7, no. 2, p. S97, Jan. 2005.
- [13] C. R. Williams, S. R. Andrews, S. A. Maier, A. I. Fernández-Domínguez, L. Martín-Moreno, and F. J. García-Vidal, "Highly confined guiding of terahertz surface plasmon polaritons on structured metal surfaces," *Nature Photon.*, vol. 2, pp. 175–179, Mar. 2008.
- [14] S. A. Maier, S. R. Andrews, L. Martín-Moreno, and F. J. García-Vidal, "Terahertz surface plasmon-polariton propagation and focusing on periodically corrugated metal wires," *Phys. Rev. Lett.*, vol. 97, Oct. 2006, Art. no. 176805.
- [15] L. Liu, Z. Li, P. Ning, B. Xu, C. Chen, J. Xu, X. Chen, and C. Gu, "Deep-subwavelength guiding and superfocusing of spoof surface plasmon polaritons on helically grooved metal wire," *Plasmonics*, vol. 11, no. 2, pp. 359–364, Apr. 2016.
- [16] L. Liu, Z. Li, P. Ning, B. Xu, C. Gu, C. Chen, J. Yan, Z. Niu, and Y. Zhao, "Smooth bridge between guided waves and spoof surface plasmon polaritons," *Opt. Lett.*, vol. 40, no. 8, pp. 1810–1813, Apr. 2015.
- [17] J. J. Wu, C. J. Wu, J. Q. Shen, D. J. Hou, and W. C. Lo, "Properties of transmission and leaky modes in a plasmonic waveguide constructed by periodic subwavelength metallic hollow blocks," *Sci. Rep.*, vol. 5, Sep. 2015, Art. no. 14461.
- [18] A. I. Fernández-Domínguez, F. J. García-Vidal, D. Martín-Cano, L. Martín-Moreno, E. Moreno, and M. L. Nesterov, "Domino plasmons for subwavelength terahertz circuitry," *Opt. Express*, vol. 18, no. 2, pp. 754–764, Jan. 2010.
- [19] D. Martín-Cano, O. Quevedo-Teruel, E. Moreno, L. Martín-Moreno, and F. J. García-Vidal, "Waveguided spoof surface plasmons with deep-subwavelength lateral confinement," *Opt. Lett.*, vol. 36, no. 23, pp. 4635–4637, Dec. 2011.
- [20] B. Gupta, S. Pandey, and A. Nahata, "Plasmonic waveguides based on symmetric and asymmetric T-shaped structures," *Opt. Express*, vol. 22, no. 3, pp. 2868–2880, Feb. 2014.
- [21] A. I. Fernández-Domínguez, E. Moreno, L. Martín-Moreno, and F. J. García-Vidal, "Terahertz wedge plasmon polaritons," *Opt. Lett.*, vol. 34, no. 13, pp. 2063–2065, Jul. 2009.
- [22] J. J. Wu, D. J. Hou, H.-L. Chiueh, J.-Q. Shen, C.-J. Wu, Y.-H. Kao, W.-C. Lo, T.-J. Yang, and I.-J. Hsieh, "Kind of high directivity scanning radiation based on subwavelength periodic metal structure," *Electron. Lett.*, vol. 50, no. 22, pp. 1611–1613, 2014.
- [23] X. Shen, T. J. Cui, D. F. Martín-Cano, and J. García-Vidal, "Conformal surface plasmons propagating on ultrathin and flexible films," *Proc. Nat. Acad. Sci. USA*, vol. 110, no. 1, pp. 40–45, Jan. 2013.
- [24] X. Shen and T. J. Cui, "Planar plasmonic metamaterial on a thin film with nearly zero thickness," *Appl. Phys. Lett.*, vol. 102, no. 21, May 2013, Art. no. 211909.
- [25] H. F. Ma, X. Shen, Q. Cheng, W. X. Jiang, and T. J. Cui, "Broadband and high-efficiency conversion from guided waves to spoof surface plasmon polaritons," *Laser Photon. Rev.*, vol. 8, no. 1, pp. 146–151, 2014.
- [26] L. Ye, Y. Xiao, Y. Liu, L. Zhang, G. Cai, and Q. H. Liu, "Strongly confined spoof surface plasmon polaritons waveguiding enabled by planar staggered plasmonic waveguides," *Sci. Rep.*, vol. 6, Dec. 2016, Art. no. 38528.
- [27] L. Ye, Y. Xiao, N. Liu, Z. Song, W. Zhang, and Q. H. Liu, "Plasmonic waveguide with folded stubs for highly confined terahertz propagation and concentration," *Opt. Express*, vol. 25, no. 2, pp. 898–906, Jan. 2017.
- [28] L. Ye, W. Zhang, B. K. Ofori-Okai, W. Li, J. Zhuo, G. Cai, and Q. H. Liu, "Super subwavelength guiding and rejecting of terahertz spoof SPPs enabled by planar plasmonic waveguides and notch filters based on spiral-shaped units," *J. Lightw. Technol.*, vol. 36, no. 20, pp. 4988–4994, Oct. 15, 2018.
- [29] Y. J. Zhou and B. J. Yang, "Planar spoof plasmonic ultra-wideband filter based on low-loss and compact terahertz waveguide corrugated with dumbbell grooves," *Appl. Opt.*, vol. 54, no. 14, pp. 4529–4533, 2015, doi: 10.1364/AO.54.004529.
- [30] J. Y. Yin, J. Ren, Q. Zhang, H. C. Zhang, Y. Q. Liu, Y. B. Li, X. Wan, and T. J. Cui, "Frequency-controlled broad-angle beam scanning of patch array fed by spoof surface plasmon polaritons," *IEEE Trans. Antennas Propag.*, vol. 64, no. 12, pp. 5181–5189, Dec. 2016.
- [31] D. Liao, Y. Zhang, and H. Wang, "Wide-angle frequency-controlled beam-scanning antenna fed by standing wave based on the cutoff characteristics of spoof surface plasmon polaritons," *IEEE Antennas Wireless Propag. Lett.*, vol. 17, no. 7, pp. 1238–1241, Jul. 2018.

- [32] S. Zhou, J.-Y. Lin, S.-W. Wong, F. Deng, L. Zhu, Y. Yang, Y. He, and Z.-H. Tu, "Spoof surface plasmon polaritons power divider with large isolation," *Sci. Rep.*, vol. 8, no. 1, Apr. 2018, Art. no. 5947.
- [33] J. Luo, J. He, A. Apriyana, G. Feng, Q. Huang, and Y. P. Zhang, "Tunable surface-plasmon-polariton filter constructed by corrugated metallic line and high permittivity material," *IEEE Access*, vol. 6, pp. 10358–10364, 2018.
- [34] Y. J. Zhou and Q. X. Xiao, "Electronically controlled rejections of spoof surface plasmons polaritons," *J. Appl. Phys.*, vol. 121, no. 12, Mar. 2017, Art. no. 123109.
- [35] D. Zhang, K. Zhang, Q. Wu, G. Yang, and X. Sha, "High-efficiency broadband excitation and propagation of second-mode spoof surface plasmon polaritons by a complementary structure," *Opt. Lett.*, vol. 42, no. 14, pp. 2766–2769, Jul. 2017.
- [36] Z. Xu, S. Liu, S. Li, H. Zhao, L. Liu, and X. Yin, "Tunneling of spoof surface plasmon polaritons through magnetoinductive metamaterial channels," *Appl. Phys. Express*, vol. 11, no. 4, Mar. 2018, Art. no. 042002.
- [37] D. Deslandes and K. Wu, "Integrated microstrip and rectangular waveguide in planar form," *IEEE Microw. Wireless Compon. Lett.*, vol. 11, no. 2, pp. 68–70, Feb. 2001.
- [38] Y. Cassivi and K. Wu, "Low cost microwave oscillator using substrate integrated waveguide cavity," *IEEE Microw. Wireless Compon. Lett.*, vol. 13, no. 2, pp. 48–50, Feb. 2003.
- [39] W. Hong, K. Wu, H. Tang, J. Chen, P. Chen, Y. Cheng, and J. Xu, "SIW-like guided wave structures and applications," *IEICE Trans. Electron.*, vol. 92, no. 9, pp. 1111–1123, Sep. 2009.
- [40] X.-P. Chen and K. Wu, "Substrate integrated waveguide filter: Basic design rules and fundamental structure features," *IEEE Microw. Mag.*, vol. 15, no. 5, pp. 108–116, Jul. 2014.
- [41] Q. Zhang, H. C. Zhang, H. Wu, and T. J. Cui, "A hybrid circuit for spoof surface plasmons and spatial waveguide modes to reach controllable bandpass filters," *Sci. Rep.*, vol. 5, Nov. 2015, Art. no. 16531.
- [42] J. F. Zhu, S. W. Liao, S. F. Li, and Q. Xue, "Half-spaced substrate integrated spoof surface plasmon polaritons based transmission line," *Sci. Rep.*, vol. 7, no. 1, Aug. 2017, Art. no. 8013.
- [43] A. Niembro-Martín, V. Nasserddine, E. Pistono, H. Issa, A.-L. Franc, T.-P. Vuong, and P. Ferrari, "Slow-wave substrate integrated waveguide," *IEEE Trans. Microw. Theory Techn.*, vol. 62, no. 8, pp. 1625–1633, Aug. 2014.
- [44] D.-F. Guan, P. You, Q. Zhang, Z. B. Yang, H. Liu, and S. W. Yong, "Slow-wave half-mode substrate integrated waveguide using spoof surface plasmon polariton structure," *IEEE Trans. Microw. Theory Techn.*, vol. 66, no. 6, pp. 2946–2952, Jun. 2018.
- [45] K. Rudramuni, K. Kandasamy, A. Kandwal, and Q. Zhang, "Compact bandpass filter based on hybrid spoof surface plasmon and substrate integrated waveguide transmission line," in *Proc. IEEE Elect. Desing Adv. Packag. Syst. Symp.*, Haining, China, Dec. 2017, pp. 1–3.
- [46] P. Chen, L. Li, K. Yang, and Q. Chen, "Hybrid spoof surface plasmon polariton and substrate integrated waveguide broadband bandpass filter with wide out-of-band rejection," *IEEE Microw. Wireless Compon. Lett.*, vol. 28, no. 11, pp. 984–986, Nov. 2018.
- [47] Z.-B. Yang, D.-F. Guan, Q. Zhang, P. You, X.-X. Hou, S.-D. Xu, and S.-W. Yong, "A hybrid substrate-integrated waveguide and spoof surface plasmon-polariton one-layer dual bandpass filter formed by resonant tunneling effect," *Appl. Phys. Express*, vol. 11, no. 11, Oct. 2018, Art. no. 114101.



YAO CHEN received the B.S. degree in telecommunications engineering from the Nanjing University of Science and Technology, Nanjing, China, in 2016. She is currently pursuing the M.E. degree with Xiamen University, Xiamen, China. Her current research interests include microwave components and spoof surface plasmon polariton waveguides.



KAI DA XU (S'13–M'15–SM'18) received the B.S. and Ph.D. degrees in electromagnetic field and microwave technology from the University of Electronic Science and Technology of China (UESTC), Chengdu, China, in 2009 and 2015, respectively.

From 2012 to 2014, he was a Visiting Researcher with the Department of Electrical and Computer Engineering, Duke University, Durham, NC, USA. From 2016 to 2017, he was a Postdoctoral Fellow with the State Key Laboratory of Millimeter Waves, City University of Hong Kong, Hong Kong. In 2015, he joined the Department of Electronic Science, Xiamen University, Xiamen, China, as an Assistant Professor. Since 2018, he has been an Honorary Fellow with the Department of Electrical and Computer Engineering, University of Wisconsin–Madison, WI, USA. He has authored or coauthored over 100 papers in peer-reviewed journals and conference proceedings. His current research interests include RF/microwave and mm-wave devices, antenna arrays, and nanoscale memristors.

Dr. Xu received the UESTC Outstanding Graduate Awards, in 2009 and 2015, respectively. He was a recipient of the National Graduate Student Scholarship from the Ministry of Education, China, in 2012, 2013, and 2014, respectively. He is serving as a Reviewer for the several IEEE and IET journals, including the IEEE TRANSACTIONS ON MICROWAVE THEORY AND TECHNIQUES, the IEEE TRANSACTIONS ON ANTENNAS AND PROPAGATION, the IEEE TRANSACTIONS ON ELECTRON DEVICES, the IEEE TRANSACTIONS ON CIRCUITS AND SYSTEMS II-EXPRESS BRIEFS, the IEEE TRANSACTIONS ON COMPUTER-AIDED DESIGN OF INTEGRATED CIRCUITS AND SYSTEMS, the IEEE ANTENNAS AND WIRELESS PROPAGATION LETTERS, the IEEE MICROWAVE AND WIRELESS COMPONENTS LETTERS, the IEEE Microwave Magazine, IEEE ACCESS, IET Microwaves, Antennas & Propagation, and Electronics Letters. Since 2017, he has been an Associate Editor of IEEE ACCESS and Electronics Letters. He is also an Editorial Board Member of the AEU-International Journal of Electronics and Communications.



China. He has published over 70 papers in peer-reviewed journals and conference proceedings. His current research interests include microwave and terahertz waveguides, circuits and antennas, plasmonics, metamaterials, and graphene-based devices.

LONGFANG YE received the Ph.D. degree in electromagnetic field and microwave technology from the University of Electronic Science and Technology of China, Chengdu, China, in 2013. From 2011 to 2013, he was a Visiting Student with the Massachusetts Institute of Technology, Cambridge, MA, USA. He is currently an Assistant Professor with the Institute of Electromagnetics and Acoustics and the Department of Electronic Science, Xiamen University, Xiamen,



WEIWEN LI received the B.S. degree in electronic engineering from Jilin University, Changchun, China, in 1993, and the M.S. degree in material engineering and the Ph.D. degree in electronic engineering from Zhejiang University, Hangzhou, China, in 2002 and 2005, respectively. He is currently an Associate Professor of electronic engineering with Xiamen University, China. His research interests include the electromagnetic wave theory and microwave technology.



QING HUO LIU (S'88–M'89–SM'94–F'05) received the B.S. and M.S. degrees in physics from Xiamen University, China, and the Ph.D. degree in electrical engineering from the University of Illinois at Urbana–Champaign.

He was with the Electromagnetics Laboratory with the University of Illinois at Urbana–Champaign as a Research Assistant, from 1986 to 1988, and as a Postdoctoral Research Associate, from 1989 to 1990. He was a Research

Scientist and a Program Leader with the Schlumberger-Doll Research, Ridgefield, CT, USA, from 1990 to 1995. From 1996 to 1999, he was an Associate Professor with New Mexico State University. Since 1999, he has been with Duke University, where he is currently a Professor of electrical and computer engineering. He has published over 450 papers in refereed journals and 550 papers in conference proceedings. His research interests include computational electromagnetics and acoustics, inverse problems, and their application in nanophotonics, geophysics, biomedical imaging, and electronic packaging.

Dr. Liu is a Fellow of the IEEE, the Acoustical Society of America, the Electromagnetics Academy, and the Optical Society of America. He received the 1996 Presidential Early Career Award for Scientists and Engineers (PECASE) from the White House, the 1996 Early Career Research Award from the Environmental Protection Agency, and the 1997 CAREER Award from the National Science Foundation. He received the 2017 Technical Achievement Award and the 2018 Computational Electromagnetics Award from the Applied Computational Electromagnetics Society and the 2018 Harrington-Mitra Award in Computational Electromagnetics from the IEEE Antennas and Propagation Society. He has served as an IEEE Antennas and Propagation Society Distinguished Lecturer. He currently serves as the Founding Editor-in-Chief of the new IEEE JOURNAL ON MULTISCALE AND MULTIPHYSICS COMPUTATIONAL TECHNIQUES.



YONG ZHANG received the B.S., M.S., and Ph.D. degrees from the University of Electronic Science and Technology of China (UESTC), Chengdu, China, in 1999, 2001, and 2004, respectively. He was invited as a Senior Visiting Scholar with Harvard University, in 2018. He has been working in the field of microwave engineering for 20 years, since he entered UESTC as a master's student. He is currently a Professor with UESTC because of his outstanding research achievements. He has

published more than 100 journal and conference papers. He has applied 18 patents and six of them got the authorization. His current research interests include the design and application of passive and active components at microwave and millimeter-wave frequencies and solid-state terahertz technology.

• • •